

Selective Catalytic Reduction of Nitric Oxide by Ammonia: The Activation Mechanism

Yuka Kobayashi,* Nobuo Tajima, Haruyuki Nakano, and Kimihiko Hirao

Department of Applied Chemistry, School of Engineering, The University of Tokyo,
Hongo 7-3-1, Bunkyo-ku, Tokyo, 113-8656 Japan

Received: May 12, 2004; In Final Form: June 25, 2004

The activation mechanism of NH_3 in the selective catalytic reduction of NO by NH_3 on a $\text{V}_2\text{O}_7\text{H}_4$ cluster was investigated using a complete active space self-consistent field method. Because of the easy bond dissociation of NH_4^+ adsorbed on Brønsted acid sites of the V_2O_5 configuration, the radical species NH_3^+ can occur with an activation energy of only 26.7 kcal/mol. The highly active intermediate NH_3^+ is stabilized by forming a very strong hydrogen bond of approximately 29.2 kcal/mol to the vanadyl oxygen. This stabilization mechanism is very similar to the low-barrier hydrogen bond in the transition state, or in an unstable intermediate state, which has been reported for some enzymatic reactions.

In recent decades, the problem of air pollution and acid rain, caused by toxic gases such as NO_x and SO_x , has become ecologically serious.¹ The technique of decomposing NO_x with the selective catalytic reduction (SCR) of NO by NH_3 over vanadia-based catalysts is very effective. This method, which was established in the 1970s, is still the major strategy for the reduction of NO industrially. Therefore, considerable effort has been spent in elucidating the reaction processes of the SCR, and many different schemes have been suggested in the literature.² However, the development of a next-generation catalyst demands a deep understanding of the reaction mechanisms of the SCR.

Experiments have proven that NO and N_2 are only weakly adsorbed on a V_2O_5 surface. In contrast, NH_3 has been reported to be readily adsorbed on the surface of Brønsted acid sites of V_2O_5 .^{3,4} These observations lead to the conclusion that the SCR reaction can be described by the Eley–Rideal mechanism involving adsorbed NH_3 species and gas-phase NO.⁵ The experimental evidence has been that both the V–OH (Brønsted acid sites) and the V=O species of a V_2O_5 surface are crucial for conversion of NO_x .⁶ In situ Fourier transform IR (FTIR) and on-line mass spectroscopic studies have shown that NH_4^+ is the predominant species on vanadia/titania catalysts under SCR conditions.⁷ However, no direct observation of a NO-reacting species has been reported in any experiment. The identification of the active species is clearly one of the most important, and challenging, subjects left in order to explain the reaction mechanism of SCR. NH_3 adsorbed at Brønsted acid sites has been reported to form NH_4^+ species.⁷ This suggests that the adsorbed ammonia never interacts directly with NO. At high temperatures (>300 °C), NH_2 is considered to be the activated species in the thermal decomposition of NO.⁸ Because NH_2NO , which is produced when NH_2 and NO combine, has never been detected under SCR conditions on a V=O, it cannot be considered a key molecule.⁹ NH_4^+ and NH_3^+ have been suggested as the activated species in SCR.^{10,6} Recently, our group investigated the reactivity of NH_4^+ and NH_3^+ with NO under gas-phase conditions using a second-order multireference

perturbation method.¹¹ In that study, a large difference in the energy profile of the initial N–N bond formation step was observed. In the first N–N bond intermediate produced by NH_4^+ and NO, the N–N bond is very unstable because one electron occupies its antibonding orbital. Therefore, a large amount of energy (71.4 kcal/mol) is required to form the N–N bond complex, which indicates a low reactivity. Conversely, NO reacts with NH_3^+ exothermically and forms a relatively stable N–N coordination bond, where the radical electron is transferred from NO to NH_3^+ . The resulting complex is produced without any activation barrier so that NH_3^+ is expected to decompose NO efficiently on the V_2O_5 surface. However, in the gas phase, NH_3^+ has a much higher total energy than NH_4^+ . In the present study, we theoretically investigated these total energies at the V_2O_5 surface model.

Recently several groups are investigating the behavior of NH_4^+ on the catalyst. A wide range of adsorption energy of NH_4^+ is proposed on the basis of various surface models, e.g., VO_3H_3 , $\text{V}_2\text{O}_7\text{H}_4$, $\text{V}_2\text{O}_9\text{H}_8$, and $\text{V}_4\text{O}_{16}\text{H}_{12}$, etc., using various theoretical methods.¹² However, crystal structure shows that the coordination environment of the V atom is tetrahedral and that the oxidation number is +5.¹³ The simple $\text{V}_2\text{O}_7\text{H}_4$ cluster model is more reasonable to describe the (010) surface of the V_2O_5 crystal, although this model has never been reported successful adsorption energy of NH_4^+ so far. The difficulty in modeling this system originates from the V=O double bond. A complicated electronic structure arises because of the d orbitals of the V atom. A complete active-space self-consistent field method (CASSCF) represents the π -bonding system in a manner that allows the electrostatic correlation to be treated with high accuracy.¹⁴ The breakdown of the mean-field approximation, which was observed in applying Hartree–Fock (HF) and density functional theory (DFT), can be avoided. We herein demonstrate the adsorption energy and possibility of the existence of unstable intermediate, NH_3^+ , on the surface using $\text{V}_2\text{O}_7\text{H}_4$ model by means of the method based on multiconfiguration.

Computational Details

All geometries, which are not defined in the text, were optimized using 3-21G basis sets.¹⁵ The determined structures were evaluated using the following basis sets: SBKJC VDZ

* To whom correspondence may be addressed. E-mail: yuka@chiral.t.u-tokyo.ac.jp. Fax: +81-3-5841-7267. Current address: Department of Chemistry and Biotechnology, School of Engineering, The University of Tokyo, Hongo 7-3-1, Bunkyo-ku, Tokyo 113-8656, Japan.

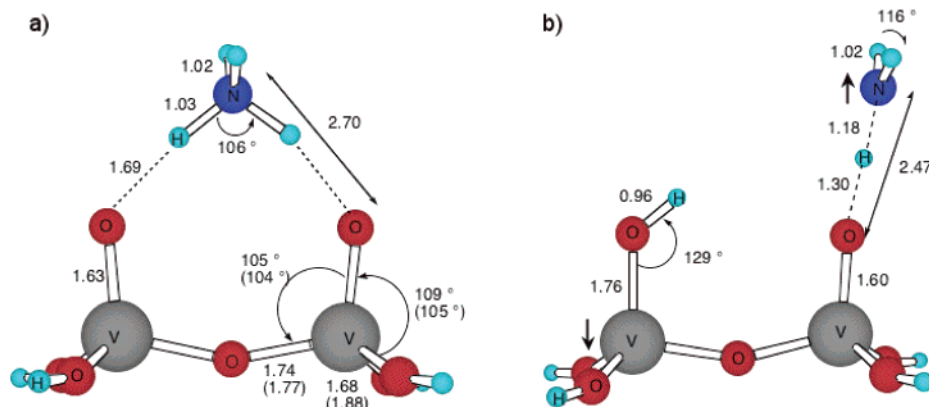


Figure 1. The adsorption structures of NH_4^+ and NH_3^+ on a $\text{V}_2\text{O}_7\text{H}_4$ cluster are shown in (a) and (b), respectively. Bond lengths are shown in angstroms, and the angles in parentheses show experimental values. Bold arrows mean electron spins and hushed lines show hydrogen bonds. (a) The NH_4^+ adsorbs in a nearly symmetrical fashion at the two $\text{V}=\text{O}$ sites (Brønsted acid sites) by hydrogen bonds. (b) After dissociation, the NH_3^+ stands on the $\text{V}=\text{O}$ site with a strong hydrogen bond.

ECP plus polarization for the V atoms;¹⁶ cc-pVDZ for the O atoms of $\text{V}=\text{O}$ sites;¹⁷ cc-pVDZ for the N and H atoms of the NH_4^+ and NH_3^+ ; 3-21G for all other atoms. For the $\text{V}_2\text{O}_7\text{H}_4$ cluster, the active space was chosen as [8e,8o], which includes 2 pairs of $d\pi$ orbitals for each $\text{V}=\text{O}$ site. For the supermolecule of NH_4^+ on the $\text{V}_2\text{O}_7\text{H}_4$ cluster, [12e,12o], namely, [4e,4o] for two N–H bonds of the NH_4^+ which are in interaction with the $\text{V}=\text{O}$, and [8e, 8o] for the two $\text{V}=\text{O}$ sites was chosen. All calculations were performed using the ab initio quantum chemistry package GAMESS.¹⁸

Results and Discussion

To examine the bonding property of $\text{V}=\text{O}$, we calculated the $\text{V}_2\text{O}_7\text{H}_4$ cluster with CASSCF[6e,9o] /3-21G using the structures, which is determined by ROHF/3-21G in singlet and triplet, respectively.¹⁹ As a result, $\text{V}_2\text{O}_7\text{H}_4$ cluster in the singlet state is more stable as 38.5 kcal/mol than that in the triplet state. This calculation clarified that $\text{V}=\text{O}$ bond has quite multiconfigurational character in both states. The weight of the main electronic configuration is only 85%; the rest of the configuration consists of $d\pi-d\pi^*$ and $d\sigma-d\sigma^*$ contributions, even in the ground state, as shown in Table 1. The bond length of the terminal vanadyl groups ($\text{V}=\text{O}$) was reoptimized with CASSCF-[8e,8o]/3-21G and found that it was 1.63 Å. This is marginally longer than the experimental value for a V_2O_5 single crystal (1.58 Å), measured by X-ray diffraction.¹³ Theoretical investigations on vanadyl, which is 3-fold and 4-fold coordinated with oxygen, show only marginal changes in the $\text{V}=\text{O}$ bond length. The difference of adsorption energy between the experimental and theoretical results is a good measure for estimating the quality of a calculation. CASSCF[12e,12o] yields $E_{\text{ads}}(\text{NH}_4^+) = 24.7$ kcal/mol as the NH_4^+ adsorption energy to the $\text{V}_2\text{O}_7\text{H}_4$ cluster, which is in good agreement with 18–26 kcal/mol, observed in the experiment.²⁰ On the other hand, DFT gives too large adsorption energy for $\text{V}_2\text{O}_7\text{H}_4$; the values are in ~50–60 kcal/mol, although it gives a reasonable value for $\text{V}_2\text{O}_9\text{H}_4$, in which V^{5+} is not preserved.

The potential-energy surface (PES) of the reaction $\text{NH}_4^+ \rightarrow \text{NH}_3^+ + \text{H}$ in the gas phase was investigated using CASSCF-[8e,8o]/cc-pVDZ prior to the surface reaction.²¹ This revealed that the potential energy increased monotonically with the NH_3^+ to H distance, that there was no transition state to produce NH_3^+ , and also that the energy difference between the reactant NH_4^+ and the product ($\text{NH}_3^+ + \text{H}$) is as large as ($E_{\text{diss(gas)}} = 123.7$

TABLE 1: Main and Minor Configurations in CASSCF[6e,9o] Wavefunctions of the $\text{V}_2\text{O}_7\text{H}_4$ Cluster in Singlet and Triplet States

	major configuration ^a	ratio (%)	major configuration ^b	ratio (%)
$\text{V}_2\text{O}_7\text{H}_4$ (singlet)	$d\pi(2)$	84.9	$d\pi(2) \rightarrow d\pi^*(1)$	1.7
	$d\sigma(2)$		$d\pi(2) \rightarrow d\pi^*(1)$	1.2
	$d\pi(2)$		$d\sigma(2) \rightarrow d\sigma^*(1)$	1.1
			$d\pi(2) \rightarrow d\pi^*(1)$	1.1
			$d\sigma(2) \rightarrow d\sigma^*(1)$	1.0
			$d\pi(2) \rightarrow d\pi^*(1)$	1.0
$\text{V}_2\text{O}_7\text{H}_4$ (triplet)	$d\pi(2)$	19.0	$d\sigma(2) \rightarrow \text{O}:2p(1)$	22.1
	$d\sigma(2)$		$d\pi(2) \rightarrow \text{O}:2p(1)$	10.0
	$\text{O}:2p(1)$		$d\sigma(2) \rightarrow \text{V}:3d(1)$	8.6
	$\text{V}:3d(1)$		$d\sigma(2) \rightarrow \text{V}:3d(1)$	7.5
			$d\pi(2) \rightarrow \text{O}:2p(1)$	1.3
			$d\sigma(2) \rightarrow \text{O}:2p(1)$	1.3
			$d\sigma(2) \rightarrow \text{V}:3d(1)$	1.2
			$d\pi(2) \rightarrow \text{O}:2p(1)$	1.2
			$d\pi(2) \rightarrow d\pi^*(1)$	1.1

^a The occupied electron numbers are shown in parentheses. ^b Parentheses mean the excitation electron numbers from the main configurations. For example, $d\pi(2) \rightarrow d\pi^*(1)$ means one electron excitation configuration from doubly occupied $d\pi$ orbital to $d\pi^*$ orbital.

kcal/mol). This corresponds to the required energy for the production of NH_3^+ in the gas phase, on an obviously unstable state.

Next, we examined the PES of NH_4^+ on the $\text{V}_2\text{O}_7\text{H}_4$ cluster. The bond dissociation of NH_4^+ on the surface was investigated with CASSCF[12e,12o] using basis sets mentioned in the computational section. The optimized structures and the energy diagram of the dissociation of NH_4^+ on the surface are displayed in Figures 1 and 2, respectively. The theoretical representation of the dissociation products $\text{V}=\text{O}\cdots\text{NH}_3^+$ and $\text{V}-\text{OH}$ are in an open-shell singlet state (Figure 1b). There is no activation barrier, which is similar to the result in the gas phase. The energy difference between the reactant and the product is $E_{\text{diss}}(\text{V}_2\text{O}_7\text{H}_4) = 51.4$ kcal/mol. Although zero-point energy and entropic effects are not included in this calculation, these effects would not have a strong influence to the result. In a solid catalytic system, the real activation energy of the reaction is reduced by the heat of adsorption of the molecules on the catalytic surface (see Figure 2).²² Under SCR conditions, NH_4^+ is the main adsorption species.¹⁰ It can be considered that most of its

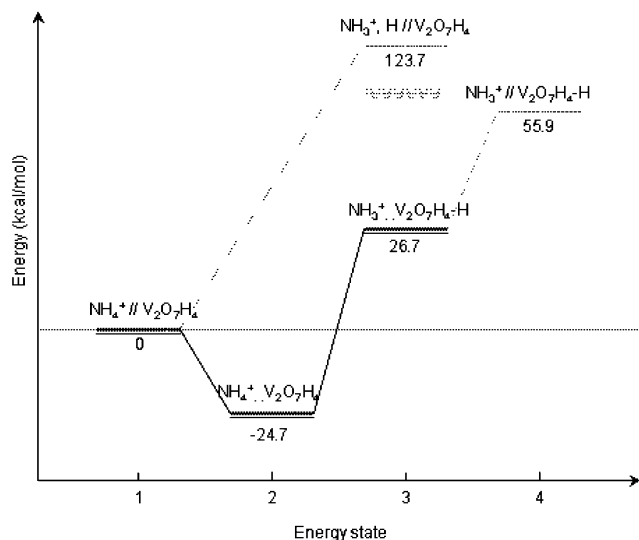


Figure 2. The energy diagram of the species on the $V_2O_7H_4$ model, calculated with CASSCF[12e,12o]/SBKJIC VDZ ECP plus polarization for the V atoms; cc-pVDZ for the O atoms of $V=O$ sites; cc-pVDZ for the N and H atoms of the NH_4^+ and NH_3^+ ; 3-21G for all other atoms. State 1 is the reference energy level. It represents a NH_4^+ molecule in the gas phase without any interaction to the $V_2O_7H_4$. State 2 represents the adsorbed NH_4^+ which relates to Figure 1a. Moving to state 3, the $V_2O_7H_4$ abstracts one hydrogen atom from the NH_4^+ . (Figure 1b depicts the new configuration in detail.) For comparison, an activation energy of $E_{\text{diss(gas)}} = 123.7$ kcal/mol would be needed for a hydrogen dissociation reaction in the gas phase. State 4 indicates the binding energy of the NH_3^+ to the $V-O$ of the $V_2O_7H_4$. The energies are defined in the text.

adsorption energy is consumed in forming the activated species NH_3^+ for the next reaction process. On the surface, a decrease of the required dissociation energy as great as $\Delta E_{\text{diss}} = E_{\text{diss(gas)}} - E_{\text{diss}(V_2O_7H_4)} = 72.3$ kcal/mol, compared with the gas phase, can be obtained. Furthermore, the drastic reduction of the activation energy down to only 26.7 kcal/mol is due to two advantageous factors (see Figure 2). One is the high hydrogen affinity to the $V=O$ site of the surface. A CASSCF [9e,8o] calculation showed this to be $E_{(VO-H)} = 43.1$ kcal/mol.²³ The other factor is the formation of a very strong hydrogen bond to the surface on the adsorption site of NH_3^+ . NH_4^+ adsorbs the two sites with ordinary hydrogen bonds, where the distance between the N atom and the O atoms of $V=O$ sites is 2.71 Å (Figure 1a). On the other hand, NH_3^+ stays on a $V=O$ site with a very strong hydrogen bond, this leads to an unusual short distance of 2.47 Å between N and O atom and an extended N—H bond (Figure 1b). The bond length of the $N\cdots H$ and the $H\cdots O$ are 1.18 and 1.30 Å, respectively. It should be noted that the $V=O$ site interacts with NH_3^+ is shrunken to 1.60 Å compared with the normal $V=O$ bond. This activation mechanism is strongly supported by in situ FTIR study,²⁴ which shows that the peaks corresponds to $V^{5+}-OH$ and $V^{4+}-OH$, although the peaks of NH_3^+ itself are difficult to be assigned. In the present system, the binding energy of the active intermediate NH_3^+ on the surface model can be calculated by $E_{\text{ads}}(NH_3^+) = \Delta E_{\text{diss}} - E_{(VO-H)}$. A remarkably high $E_{\text{ads}}(NH_3^+)$ value of 29.2 kcal/mol, which forms a strong hydrogen bond, can be obtained.

The role of the strong hydrogen bond is similar to the biological hydrogen-bonding systems reported for some biological reaction processes. The unusually short hydrogen bonds are known as low-barrier hydrogen bonds (LBHB) or as short strong hydrogen bonds. LBHB has attracted considerable interest as an important factor in accelerating biochemical reactions, for

example, in enzymes.²⁵ In several enzymatic reactions, a LBHB is formed in the enzyme—substrate complex at a transition state and/or an intermediate, where it is considered that an energy of 10–20 kcal/mol is saved, the reaction is therefore significantly assisted. For example, on vanadium haloperoxidases, it has been suggested that the hydrogen bond formed between a $V-O$ site and its coordinated amino residues is significant in the catalytic mechanism.²⁶

In this report, the energy profile of the key molecule NH_3^+ on the V_2O_5 surface in SCR was derived using an accurate ab initio molecular orbital method. The multiconfigurational character of the $V=O$ site is suitable to extract a hydrogen atom from the absorbed NH_4^+ on the surface because of its high hydrogen affinity. Because of the contribution of the LBHB energy to the activated $V=O$ site, only 26.7 kcal/mol is required to produce an activated NH_3^+ species. The role of the catalyst in SCR was revealed, and the beautiful similarity between the SCR and an enzymatic reaction mechanism with a LBHB was shown.

References and Notes

- (1) Henry, J. G.; Heinke, G. W. *Environmental Science and Engineering*; Prentice-Hall: Englewood Cliffs, NJ, 1989.
- (2) Busca, G.; Lietti, L.; Ramis, G.; Berti, F. *Appl. Catal. B* **1998**, *18*, 1.
- (3) Mitamoto, A.; Yamazaki, Y.; Hattori, T.; Inomata, M.; Murakami, Y. *J. Catal.* **1982**, *74*, 144.
- (4) Ramis, G.; Busca, G.; Bregani, F.; Forzatti, P. *Appl. Catal.* **1990**, *64*, 259.
- (5) Schneider, H.; Tschudin, S.; Schneider, M.; Wokaun, A.; Baiker, A. *J. Catal.* **1994**, *147*, 5.
- (6) Topsøe, N.-Y. *Science* **1994**, *265*, 1217.
- (7) Topsøe, N.-Y.; Topsøe, H.; Dumesic, J. A. *J. Catal.* **1995**, *151*, 226.
- (8) Stief, L. J.; Brobst, W. D.; Nava, D. F.; Borkowski, R. P.; Michael, J. V. *J. Chem. Soc., Faraday Trans. 2* **1982**, *78*, 1391.
- (9) Farber, M.; Harris, S. P. *J. Phys. Chem.* **1984**, *88*, 680.
- (10) Miyamoto, A.; Yamazaki, Y.; Hattori, T.; Inomata, M.; Murakami, Y. *J. Catal.* **1982**, *74*, 144.
- (11) Kobayashi, Y.; Tajima, N.; Hirao, K. *J. Phys. Chem. A* **2000**, *104*, 6855.
- (12) (a) Anstrom, M.; Topsøe, N.-Y.; Dumesic, J. A. *J. Catal.* **2003**, *213*, 115. (b) Anstrom, M.; Dumesic, J. A.; Topsøe, N.-Y. *Catal. Lett.* **2002**, *78*, 281. (c) Yin, X.; Han, H.; Miyamoto, A. *Phys. Chem. Chem. Phys.* **2000**, *2*, 4243. (d) Gilardoni, F.; Weber, J.; Baiker, A. *Int. Quantum Chem.* **1997**, *61*, 683. (e) Gilardoni, F.; Weber, J.; Baiker, A. *J. Phys. Chem. A* **1997**, *101*, 6069.
- (13) Enjalbert, R.; Galy, J. *Acta Cryst.* **1986**, *C42*, 1467.
- (14) Roos, B. O. *Int. J. Quantum Chem.* **1980**, *S14*, 175.
- (15) Binkley, J. S.; Pople, J. A.; Hehre, W. J. *J. Am. Chem. Soc.* **1980**, *102*, 939.
- (16) Stevens, W. J.; Krauss, M.; Basch, H.; Jasien, P. G. *Can. J. Chem.* **1992**, *70*, 612.
- (17) Dunning, T. H., Jr. *J. Chem. Phys.* **1989**, *90*, 1007.
- (18) Schmidt, M. W.; Baldridge, K. K.; Boatz, J. A.; Elbert, S. T.; Gordon, M. S.; Jensen, J. H.; Koseki, S.; Matsunaga, N.; Nguyen, K. A.; Su, S. J.; Windus, T. L.; Dupuis, M.; Montgomery, J. A. *J. Comput. Chem.* **1993**, *14*, 1347.
- (19) The active space includes 3 pairs of electrons in 9 orbitals of one terminal $V-O$ site in $V_2O_7H_4$ cluster to compare the energies between the two sites consistently. The $V-O$ bonds optimized with ROHF/3-21G are 1.54 Å in singlet, a value that is in good agreement with the experimental value (1.58 Å) and 1.83 Å in the triplet state.
- (20) Srmak, T. Z.; Dumesic, J. A.; Clausen, B. S.; Tornguist, E.; Topsøe, N.-Y. *J. Catal.* **1991**, *135*, 246.
- (21) The active space was chosen as [8e,8o], which includes all valence orbitals of the NH_4^+ .
- (22) Hinshelwood, C. N. *The Kinetics of Chemical Change in Gaseous Systems*; Oxford University Press: New York, 1926.
- (23) The active space was that mentioned in the computational section plus additional one electron for the H atom.
- (24) Topsøe, N.-Y.; Dumesic, J. A.; Topsøe, H. *J. Catal.* **1995**, *151*, 241.
- (25) (a) Frey, P. A. *Science* **1995**, *269*, 104. (b) Cleland, W. W.; Kreevoy, M. M. *Science* **1994**, *264*, 1927.
- (26) Butler, A. *Coord. Chem. Rev.* **1999**, *87*, 17.